Available online at www.sciencedirect.com
SCIENCE DIRECT®
Journal of Magnetic Resonance 159 (2002) 126–136
JMR Journal of Magnetic Resonance
www.academicpress.com

Large angle jumps of small molecules in amorphous matrices analyzed by 2D exchange NMR

P. Medick,[a] M. Vogel,[b] and E. Rössler[a,*]

[a] *Physikalisches Institut, Universität Bayreuth, 95440 Bayreuth, Germany*
[b] *Department of Chemical Engineering, University of Michigan, USA*

Received 12 March 2002; revised 17 October 2002

Abstract

The reorientation dynamics of deuterated benzene and hexamethyl benzene as additives to the glass former oligostyrene is studied below the glass transition temperature T_g. By means of 2D ^{2}H NMR, analyzed in the frequency and in the time domain, it is shown that the dynamics of the small molecules is governed by an isotropic large angle reorientation process, which is close to the random jump model. Furthermore, the dynamics is characterized by a broad distribution of correlation times. Even 65 K below T_g, a fraction of small molecules reorients on the timescale of 100 ms. In contrast, small angle reorientation dominates in the neat glass former polystyrene near T_g. As a consequence of the presence of large angle jumps, the 2D spectra can be described by an additive superposition of two sub-spectra—a ridge along the diagonal and a complete exchange pattern—where the weighting factor $W(t_m)$ is directly given by the reorientational correlation function $F_2(t_m)$. Additionally, for a sample with very low benzene concentration ($c \approx 0.5\%$), the 1D spectra indicate that the same dynamic scenario is present in the single particle limit. Tentatively, we assume that the large angle reorientation of the small molecules is associated with a translational diffusion process of the small molecules within the amorphous matrix.

1. Introduction

2D exchange NMR has become a major source to reveal detailed information about the mechanism of slow molecular reorientation in condensed matter. Two methods for analyzing the 2D data are established: visualization as 2D spectra [1,2] and analyzing the loss of correlation in the time domain [3]. For example, the latter approach has recently been applied to unravel the motional mechanism of the primary relaxation process (α-process) in supercooled liquids and polymers [4–8]. In these systems, the molecular reorientation is close to the limit of rotational diffusion, i.e., reorientation occurs predominantly by small angle steps, a motional mechanism discussed since long. In order to clarify the nature of the motional non-uniformities in disordered systems, often also called dynamical heterogeneities, higher order NMR methods have been applied [5,6,9]. It has been shown that the dynamical heterogeneities, characteristic of the α–process in these systems, are transient in nature, i.e., one observes exchange processes among fast and slowly reorienting molecules and both exchange and reorientation occur essentially on the same timescale. Applying 2D NMR to study the secondary relaxation processes in glasses, it has been found that dynamics is associated with highly hindered reorientation [10,11].

Another field of activity is the investigation of binary glass formers. When considering systems consisting of components, which differ in molecular size, the motion of the smaller molecules is characterized by more pronounced dynamical heterogeneities than the dynamics in neat glass formers [8,12,13]. These motional heterogeneities are most directly observed close to the glass transition temperature T_g and manifest themselves in NMR spectra composed of two spectral contributions. One is a powder spectrum of molecules immobile on a timescale of some 10 μs, the other is a central line resulting from sufficiently fast isotropically reorienting molecules, as found in liquids. An example is shown in

* Corresponding author. Fax: +49-921-552621.
E-mail address: ernst.roessler@uni-bayreuth.de (E. Rössler).

1090-7807/02/$ - see front matter © 2002 Elsevier Science (USA). All rights reserved.
PII: S1090-7807(02)00100-3

Fig. 1a where the 1D spectra of hexamethyl benzene-d_{18} in oligostyrene ($m_w = 990$ g/mol) are compiled. A central line below the glass transition temperature of the mixed system ($T_g = 297$ K) indicates that even in a basically rigid matrix a fast isotropic reorientation of a fraction of the small molecules takes place. Similar spectra are observed for other binary low molecular weight glass formers when applying ^{31}P NMR [13]. In all cases, the NMR spectra of the small molecules can be reproduced by an additive superposition of the two mentioned spectral contributions, cf. Fig. 1a.

Such spectra are called two-phase spectra [12,14,15]. In contrast, when studying the dynamics of the large molecules in these systems no such two-phase spectra show up, and the line-shape is similar to the one observed for neat glass formers [16]. In other words, for neat glass formers and for the large molecules in two component glasses the dynamical heterogeneities are significantly less pronounced than those of the small molecules.

Actually, two-phase spectra are well established for the dynamics of the diluent molecules in polymer–plasticizer systems [17,18]. However, from the above discussion it is obvious that the two-phase line shape is not a polymer effect. Rather it is always present in mixed systems provided that a certain size difference among the components exists. Not only molecular size mismatches but also differences in the glass transition temperatures of the corresponding neat systems may play a role [17,18]. Only if very similar molecules, with respect to their size or T_g, constitute a binary glass former, the mixture may exhibit features close to those of a neat system [19,20]. This shows that one has to be careful when inferring the behavior of a glass former from the dynamics of small molecules dissolved in that glass former.

The quantitative analysis of two-phase spectra has been performed by applying different models. On the one hand, within a lattice model applied for polymer–plasticizer systems bimodal dynamics has been assumed. In addition to small molecules close to the polymer chain, it is assumed that there are microclusters of mobile molecules [21], presumably undergoing Brownian rotational diffusion already below T_g. On the other hand, based on 2D spectra of a series of binary low and high molecular weight systems we have concluded that the dynamics of the small molecules is determined by a broad distribution of correlation times [5,13]. Thus, no truly immobilized small molecules exist close to T_g.

Furthermore, we have proven that there occur exchange processes between fast and slowly reorienting small molecules [5,12,13]. In binary glasses such exchange processes can be detected in a 2D experiment because the motional non-uniformities show up already in the 1D spectrum (cf. Fig. 1b), thus allowing to select a dynamically distinct sub-ensemble of molecules. In Fig. 2 a typical result of these experiments is shown. Whereas

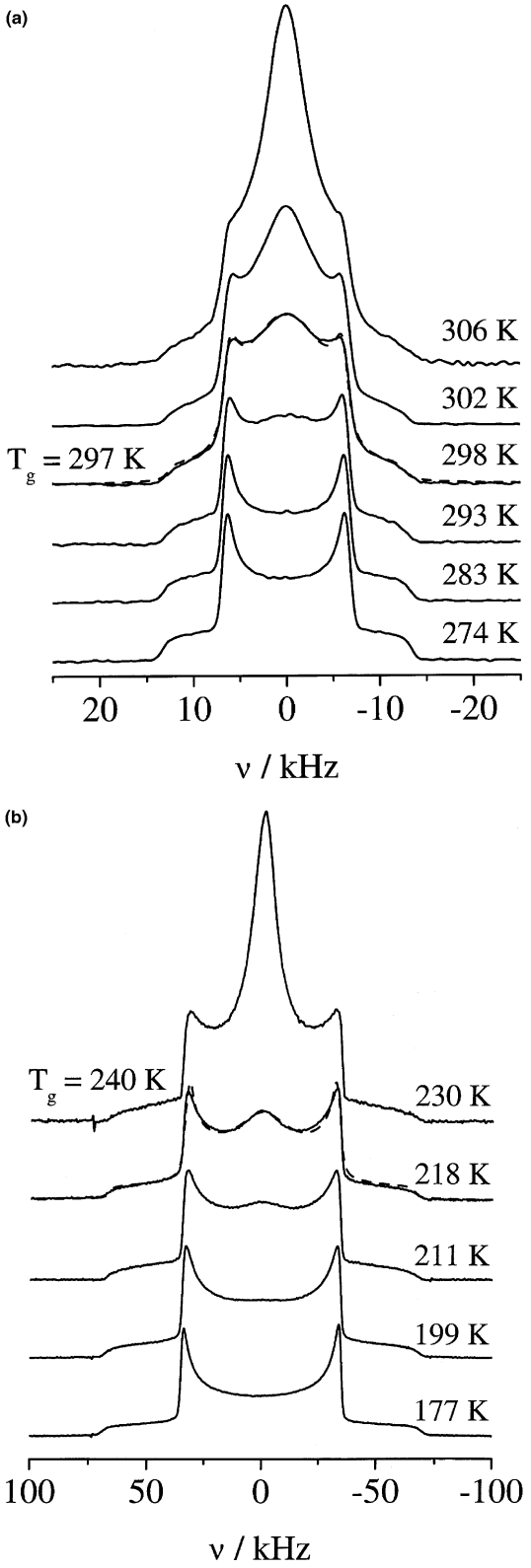

Fig. 1. (a) 1D ^2H spectra of 3.6% hexamethyl benzene-d_{18}/OS ($m_w = 990$ g/mol). (b) 1D ^2H spectra of 26% benzene-d_6/OS ($m_w = 1020$ g/mol). Dashed lines: fits according to the superposition model (cf. text).

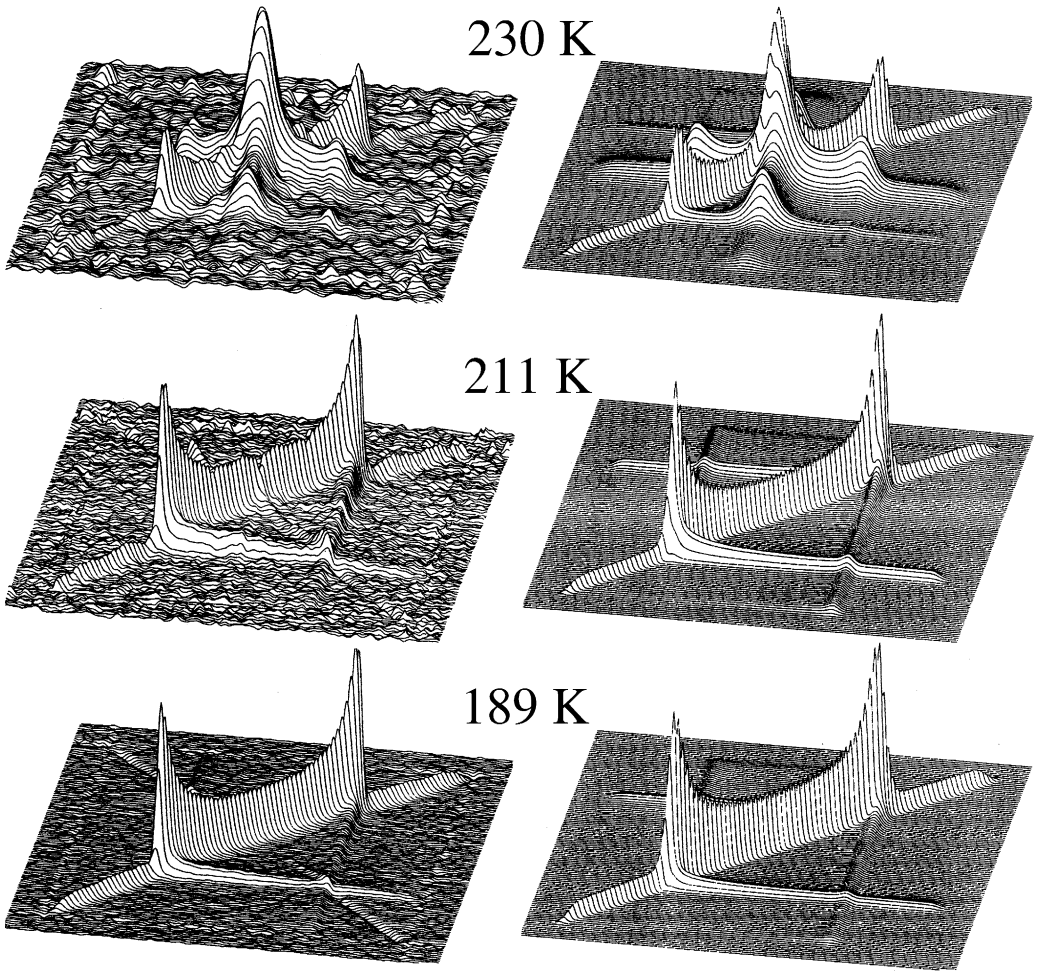

Fig. 2. 2D ^{2}H spectra of 26% benzene-d_6/OS ($m_w = 1020$ g/mol, $t_m = 100$ ms, $T_g = 240$ K) for three temperatures and corresponding isotropic random jump simulations (on the right-hand side).

the spectrum at $T = 189$ K is described by assuming isotropic reorientation on the 100 ms timescale, the spectrum at $T = 230$ K shows additional intensities along the frequency axes ($(0, \omega_2)$ and $(\omega_1, 0)$) and a peak at the center. From the latter spectrum it can be concluded that exchange processes of the molecules—between a fast and a slowly reorientation state with respect to 10 μs—take place well below $T_g = 240$ K and on the timescale of 100 ms. The central peak indicates that some molecules are in the fast reorientation state.

In the present contribution we intend to clarify the motional mechanism, in particular, the geometry of the reorientation of the small molecules in binary low molecular weight glasses, and we think valuable insights into the dynamics in polymer–plasticizer systems will also emerge. For this purpose the mixed system benzene in oligostyrene is investigated by 2D ^{2}H NMR in detail. As will be shown the motional mechanism of the sixfold symmetry axes of the benzene molecules is not determined by isotropic rotational diffusion, but rather by large angle jumps close to the limit of random jumps. This behavior was anticipated in a proceeding investigation [13]. In the literature the random jump model has been discussed, however, clear evidence for this process is still missing [2]. We will demonstrate that due to the presence of large angle jumps the 2D spectra for the small molecules in binary glass formers can be analyzed by applying a very simple method. Finally, we speculate that the reorientational motion reflects translation diffusion of the small molecules in an essentially rigid glassy matrix of the large molecules.

2. Theory

In ^{2}H NMR, the quadrupolar interaction of the deuterons with the gradient of the electric field originating from the neighboring charge distribution is probed. In our case, the distribution is nearly symmetric with respect to the C–^{2}H–bond, and it is possible to determine the orientation of the bond axis with respect to the external magnetic field. More precisely, the resonance frequency (in the rotating frame) is related to the orientation of the C–^{2}H–bond by [2]:

$$\omega(\theta) = \pm\frac{\delta}{2}(3\cos(\theta)^2 - 1) = \pm\delta P_2(\cos(\theta)), \tag{1}$$

where θ is the angle between the bond axis and the external magnetic field. δ represents the quadrupolar coupling constant. P_2 stands for the second Legendre polynomial. If the quadrupolar interaction is partially averaged by fast reorientation around a molecular symmetry axis, θ will describe the angle between this axis and the external magnetic field and the effective coupling constant δ will be reduced. Since the latter scenario is valid for all measurements in the present paper, the orientation of the sixfold symmetry axis of the small molecules benzene or hexamethyl benzene is probed.

As mentioned in Section 1, there are two ways to analyze 2D data, which are sensitive on different details of the reorientational dynamics: an analysis in the time domain reveals features of the elementary step of the reorientation process, whereas an analysis in the frequency domain yields direct access to the overall geometry of the reorientation process. Both methods are based on data acquired with the Jeener–Broekaert [22] three-pulse sequence, which correlates the NMR frequencies of one molecule at two times separated by a period called the mixing time t_m. Depending on the chosen pulse lengths and phases, the echo emerging after the last pulse is given by [2] (assuming ideal pulses and neglecting relaxation processes):

$$F_2^{ss}(t_1,t_2,t_m) = \left\langle \sin\left(\int_0^{t_1}\omega(t)\,dt\right)\cdot\sin\left(\int_{t_1+t_m}^{t_1+t_m+t_2}\omega(t)\,dt\right)\right\rangle, \tag{2}$$

$$F_2^{cc}(t_1,t_2,t_m) = \left\langle \cos\left(\int_0^{t_1}\omega(t)\,dt\right)\cdot\cos\left(\int_{t_1+t_m}^{t_1+t_m+t_2}\omega(t)\,dt\right)\right\rangle. \tag{3}$$

The brackets symbolize the ensemble average over all molecules. For slow reorientation processes, motion of the molecules during the evolution period t_1 and the detection period t_2 can be neglected and the integrals can be simplified to products:

$$F_2^{ss}(t_1,t_2,t_m) = \langle \sin(\omega_1 t_1)\cdot\sin(\omega_2 t_2)\rangle, \tag{4}$$

$$F_2^{cc}(t_1,t_2,t_m) = \langle \cos(\omega_1 t_1)\cdot\cos(\omega_2 t_2)\rangle, \tag{5}$$

where $\omega_1 = \omega(t=0)$ and $\omega_2 = \omega(t=t_m)$. To get useful information about the reorientation process, an appropriate subset $\{t_1,t_2,t_m\}$ has to be chosen.

When varying t_1 and t_2 for a given mixing time t_m, subsequent 2D Fourier transformation with respect to both time functions (cf. Eqs. (4) and (5)), leads after proper combination to the 2D absorption spectrum $S(\omega_1,\omega_2,t_m)$. It visualizes the joint probability density that a molecule follows a trajectory, which "starts" at a frequency ω_1 and "ends" at a frequency ω_2. As the resonance frequency reflects the orientation, the 2D spectra reveal the distribution $R(\beta,t_m)$ of the overall reorientation angle β of the molecules during the mixing time t_m [1].

To unravel more details of the reorientation process, or strictly speaking to find an appropriate motional model, which is compatible with the measurements, the time-domain data can be analyzed. For this purpose, another subset of correlation data, defined by $t_1 = t_2$, is chosen: the correlation functions $F_2^{ss}(t_1,t_2=t_1,t_m)$ and $F_2^{cc}(t_1,t_2=t_1,t_m)$, in the following termed as $A_2^{ss}(t_1,t_m)$ and $A_2^{cc}(t_1,t_m)$. The corresponding time constants for various evolution times t_1, $\tau^{ss}(t_1)$ and $\tau^{cc}(t_1)$, depend in a characteristic way on the geometry of the reorientation [4,6,10], i.e., the evolution of the orientation during the mixing time t_m. Assuming that the motional process can be decomposed into elementary jumps (Ivanov model) [23], it is possible to describe the details of the reorientation by a distribution of elementary jump angles $P(\gamma)$ giving the probability that a jump with an angle γ occurs. In general, γ and β differ. The latter is given by the aggregate of all elementary jumps of one molecule, which take place during the mixing time t_m. The first one is the corresponding jump angle for each jump, which is taken from the distribution $P(\gamma)$. $P(\gamma)$ determines the dependence of τ^{ss} and τ^{cc} on t_1.

For $t_1 \to 0$, $A_2^{ss}(t_1,t_m)$ is proportional to the correlation function [3]:

$$F_2(t_m) = \frac{\langle P_2(\cos(\theta_1))P_2(\cos(\theta_2))\rangle}{\langle P_2(\cos(\theta_1)^2)\rangle}. \tag{6}$$

In detail, $F_2(t_m)$ is given by:

$$F_2(t_m) = \frac{5}{2\delta^2}\lim_{t_1\to 0}\frac{A_2^{ss}(t_1,t_m)}{t_1^2} \tag{7}$$

In this limit, the corresponding time constant is labeled as τ_2 in the following.

There are two scenarios, which can be regarded as limiting cases of the reorientation process: (i) isotropic rotational diffusion and (ii) isotropic reorientation by random jumps. As we will describe our data by a model, which is close to the latter scenario (ii), it is appropriate to discuss its consequences for both the 2D spectrum $S(\omega_1,\omega_2,t_m)$ and the correlation functions $A_2^{ss}(t_1,t_m)$ and $A_2^{cc}(t_1,t_m)$.

In the framework of the Ivanov model [23], i.e., regarding the reorientation process as a sequence of instantaneous jumps, it is possible to determine the fraction $W(t_m)$ of molecules, which do not reorient during the mixing time t_m. Then, the 2D spectrum is a superposition of two sub-spectra, a diagonal spectrum $S_{dia}(\omega_1,\omega_2)$ along $\omega_1 = \omega_2$, the relative intensity of which is given by $W(t_m)$, and an off-diagonal spectrum $S_{reo}(\omega_1,\omega_2,t_m)$ with the intensity $1 - W(t_m)$. Here,

$S_{\mathrm{dia}}(\omega_1,\omega_2)$ represents immobile molecules during the mixing time, while $S_{\mathrm{reo}}(\omega_1,\omega_2,t_{\mathrm{m}})$ results from molecules, which have jumped at least once during the mixing time. In general, the spectral shape of $S_{\mathrm{reo}}(\omega_1,\omega_2,t_{\mathrm{m}})$ depends on t_{m}. However, in the case of a random jump, where the reorientation after a jump is randomly chosen from all possible orientations, S_{reo} becomes independent of t_{m} and the parameter t_{m} is omitted in the following. Then, S_{reo} can be rewritten as a product of the a priori probabilities to find the frequencies ω_1 and ω_2, respectively, with the a priori probability being equal to the spectral intensity in the 1D spectrum $S(\omega)$. Therefore, for a random jump process, the 2D spectrum is given by [2]:

$$\begin{aligned} S(\omega_1,\omega_2,t_{\mathrm{m}}) &= W(t_{\mathrm{m}})S_{\mathrm{dia}}(\omega_1,\omega_2) \\ &\quad + (1-W(t_{\mathrm{m}}))S_{\mathrm{reo}}(\omega_1,\omega_2) \\ &= W(t_{\mathrm{m}})S(\omega_1)\delta(\omega_1-\omega_2) \\ &\quad + (1-W(t_{\mathrm{m}}))S(\omega_1)S(\omega_2). \end{aligned} \tag{8}$$

Thus, the 2D spectrum can easily be analyzed. It can be described by a superposition of two sub-spectra, i.e., one may say, analogously with the 1D two-phase spectra, that 2D two-phase spectra are observed.

Switching to the analysis in the time domain, the correlation function A_2^{ss} (A_2^{cc} accordingly) is determined by:

$$\begin{aligned} A_2^{\mathrm{ss}}(t_1,t_{\mathrm{m}}) &= \langle \sin(\omega_1 t_1)\cdot\sin(\omega_2 t_1)\rangle \\ &= \int\int S(\omega_1,\omega_2,t_{\mathrm{m}})\sin(\omega_1 t_1) \\ &\quad \times \sin(\omega_2 t_1)\,\mathrm{d}\omega_1\,\mathrm{d}\omega_2. \end{aligned} \tag{9}$$

In the case of random jumps, one can write $A_2^{\mathrm{ss}}(t_1,t_{\mathrm{m}})$ as a sum of three addends (cf. Eq. (8)):

$$\begin{aligned} A_2^{\mathrm{ss}}(t_1,t_{\mathrm{m}}) &= \int\int S(\omega_1)(S(\omega_2)(1-W(t_{\mathrm{m}})) \\ &\quad + W(t_{\mathrm{m}})\delta(\omega_1-\omega_2))\cdot\sin(\omega_1 t_1) \\ &\quad \times \sin(\omega_2 t_1)\,\mathrm{d}\omega_1\,\mathrm{d}\omega_2 \\ &= \int\int S(\omega_1)S(\omega_2)\sin(\omega_1 t_1) \\ &\quad \times \sin(\omega_2 t_1)\,\mathrm{d}\omega_1\,\mathrm{d}\omega_2 - W(t_{\mathrm{m}}) \\ &\quad \times \int\int S(\omega_1)S(\omega_2)\sin(\omega_1 t_1) \\ &\quad \times \sin(\omega_2 t_1)\,\mathrm{d}\omega_1\,\mathrm{d}\omega_2 + W(t_{\mathrm{m}})\int S(\omega_1) \\ &\quad \times \sin(\omega_1 t_1)^2\,\mathrm{d}\omega_1. \end{aligned} \tag{10}$$

The first addend, named $A_\infty^{\mathrm{ss}}(t_1)$, is independent of the mixing time t_{m} and it is the limit of $A_2^{\mathrm{ss}}(t_1,t_{\mathrm{m}})$ for $t_{\mathrm{m}}\to\infty$. The other two addends are proportional to $W(t_{\mathrm{m}})$. Thus, we resort Eq. (10) in the form:

$$A_2^{\mathrm{ss}}(t_1,t_{\mathrm{m}}) = A_\infty^{\mathrm{ss}}(t_1) + \Delta A(t_1)W(t_{\mathrm{m}}). \tag{11}$$

Due to this factorization of the loss of correlation (given by $\Delta A(t_1)W(t_{\mathrm{m}})$) into a t_1- and t_{m}-dependent part, the corresponding correlation times are independent of t_1 for a random jump process. A similar calculation leads to an analog result for A_2^{cc}.

In this contribution, we discuss reorientation processes in amorphous isotropic systems. Therefore, the a priori probability is given by the 1D spectrum $S(\omega)\propto[6\delta(\omega\pm\delta/2)]^{-1/2}$. For this a priori probability and in the limit of $t_1\to 0$, the integrals in Eq. (10) can be calculated, and, thus, $F_2(t_{\mathrm{m}})$ is accessible. The first two integrals yield:

$$\begin{aligned} &\int\int S(\omega_1)S(\omega_2)\omega_1\omega_2\,\mathrm{d}\omega_1\,\mathrm{d}\omega_2 \\ &\quad\propto \left(\int_{-\delta/2}^{\delta}\frac{\omega}{\sqrt{\omega+\delta/2}}\,\mathrm{d}\omega + \int_{-\delta}^{\delta/2}\frac{\omega}{\sqrt{\omega-\delta/2}}\,\mathrm{d}\omega\right)^2 \\ &\quad\propto \left(\left[(\omega-\delta)\sqrt{\omega+\frac{\delta}{2}}\right]_{-\delta/2}^{\delta} + \cdots\right)^2 = 0 \end{aligned} \tag{12}$$

and the third integral is equivalent to:

$$\begin{aligned} \int S(\omega)\omega^2\,\mathrm{d}\omega &= \left(\int_{-\delta/2}^{\delta}\frac{\omega^2}{\sqrt{6\delta}\sqrt{\omega+\delta/2}}\,\mathrm{d}\omega \right. \\ &\quad \left. + \int_{-\delta}^{\delta/2}\frac{\omega^2}{\sqrt{6\delta}\sqrt{\omega-\delta/2}}\,\mathrm{d}\omega\right) \\ &= \frac{2\delta^2}{5} \end{aligned} \tag{13}$$

Finally it follows:

$$W(t_{\mathrm{m}}) = \lim_{t_1\to 0}\frac{5}{2\delta^2}\frac{A_2^{\mathrm{ss}}(t_1,t_{\mathrm{m}})}{t_1^2}$$

Considering Eq. (7), it becomes obvious that for an isotropic random jump process, the weighting factor $W(t_{\mathrm{m}})$ resulting from the 2D two-phase spectrum is equal to the correlation function $F_2(t_{\mathrm{m}})$:

$$W(t_{\mathrm{m}}) = F_2(t_{\mathrm{m}}) \tag{14}$$

This identity of the correlation function and the weighting factor determined by a simple two component fit of the 2D spectra will be checked below.

3. Experiments

For the experiments a Bruker CXP 200 spectrometer working at a ^{2}H Larmor frequency of 46.07 MHz was used. It was equipped with a TecMAG data acquisition system. A home-built low temperature probe was placed into an Oxford static cryostat so that a temperature stability of 0.2 K was achieved.

By varying the output power of the amplifier the length of the 90° pulses was kept constant over the

whole temperature range. The 1D spectra were recorded by applying a solid-echo sequence with a standard phase cycling and an inter-pulse delay of 15 μs. The 2D data were acquired with a modified Jeener–Broekaert sequence [22,24]. Five-pulse-sequences for the 2D spectra and four-pulse-sequences for the 2D time cos–cos (cf. Eq. (5)) and sin–sin correlation (cf. Eq. (4)) experiments were implemented. A phase cycling was applied to zero out the double-quantum coherences otherwise visible for short mixing times ($t_m \lesssim 500\,\mu s$). Additionally, for the acquisition of the 2D spectra, the lengths of the pulses before and after the mixing time period were changed for the sin–sin and cos–cos experiments to a common length corresponding to the magic angle. A saturation sequence of five to eight 90° pulses followed by a recovery delay preceded each sequence. To meet these requirements the overall numbers of scans were 128 for the four-pulse-sequence and 256 for the five-pulse-sequence [24]. In the time-domain experiments, the amplitude of the stimulated echo was determined for mixing times t_m in the range from 1 μs to 10 s. The evolution time t_1 was varied from 3 to 250 μs. The delays of the additional echo pulses after the first and third pulse of the original Jeener–Broekaert sequence were 15 μs.

For the 1D spectra, at least 2048 data points with a sampling rate of 500 kHz were recorded. In order to improve the signal/noise ratio, prior to the Fourier transformation, the time-domain data was damped with an exponential function and zero filling was applied. The corresponding time constant was set to $\delta/100$ (except for the $c = 0.5\%$ system, where 3000 Hz was used to enhance the signal/noise ratio). The same procedure with 512 points was used for the 2D spectra. When combining the two sub-spectra (cos–cos and sin–sin) [2], a residual intensity along the secondary diagonal was compensated by a weighting factor, which was in the range between 0.9 and 1.04. This may be an indication that the spin-lattice relaxation functions, characterized by T_1 for the relaxation of the Zeeman state during the cos–cos experiment and characterized by T_{1Q} for the one of the spin alignment state during the sin–sin experiment, are nearly identical. Both relaxations are non-exponential.

In the sin–sin and cos–cos time-domain experiments, the echo amplitudes were taken from the mean value of the maxima and the two adjacent points. Due to the finite pulse length a positive shift (about 2 μs) of the position of the maxima, with respect to the theoretical position for infinite short pulses, was observed. In order to compensate the additional damping of the cos–cos correlation function by spin–lattice relaxation, the latter was monitored with a standard saturation recovery sequence. As it is not possible to measure the spin alignment relaxation function in an independent experiment, we assumed that both, Zeeman and spin alignment relaxation, are identically over the whole studied temperature range. This assumption is in accordance with our findings at low temperatures, cf. below.

To analyze the time-domain data, the decays $A_2^{ii}(t_1, t_m)$ were fitted to KWW functions (ii = ss for sin–sin and cc for cos–cos experiments, respectively) with an additional damping factor to describe relaxation effects:

$$A_2^{ii}(t_1, t_m) \propto \left((1 - A_\infty^{ii}(t_1)) e^{-\left(\frac{t_m}{\tau_{KWW}^{ii}}\right)^{\beta^{ii}}} + A_\infty^{ii}(t_1) \right) \times e^{-(\frac{t_m}{T_1})^{\beta_1}}. \tag{15}$$

$A_\infty^{ii}(t_1)$ was obtained from the isotropic reorientational model (cf. Eq. (9)), T_1 and β_1 from the Zeeman relaxation function assuming $T_1 = T_{1Q}$, so that the number of free parameters was reduced. The corresponding time constants were calculated according [25]:

$$\tau^{ii} = \frac{\tau_{KWW}^{ii}}{\beta^{ii}} \cdot \Gamma\left(\frac{1}{\beta^{ii}}\right) \tag{16}$$

The dependence of τ^{ii} on t_1 is a fingerprint of the reorientation dynamics. To reproduce the salient features of the $\tau^{ii}(t_1)$ curves, random walk algorithms were applied to get a corresponding elementary jump angle distribution $P(\gamma)$ for an isotropic process [7]. To reduce the number of independent fitting parameters to eight, $P(\gamma)$ was approximated by a linear interpolation of four points between 0.5° and 89.5°. This piecewise linear function was used as the distribution of jump angles for the simulations. It should be noted that the sensitivity of this method is not very high, especially in the region $\gamma > 15°$ [4,7,26], but characteristic features, e.g., the mean jump angle, can be extracted.

The oligostyrene (OS, $m_w = 990$ g/mol and $m_w = 1020$ g/mol) was purchased from Polymer Standard Service (Mainz, Germany). Polystyrene-d_3 (PS, $m_w = 200$ kg/mol) was synthesized by G. Zimmer [27] and hexamethyl benzene-d_{18} by H. Zimmermann (Heidelberg, Germany). Benzene-d_6 was bought from Aldrich. The samples were degased using a pump and freeze procedure. Afterwards, the NMR tubes were fire sealed and tempered. Differential scanning calorimetry (DSC) experiments were carried out. Due to the broadening of the glass step with respect to that of neat systems, the upper and sharp temperature onset of the step was taken to define the glass transition temperature T_g (26% benzene-d_6/OS: $T_g = 240$ K; 0.5% benzene-d_6/OS: $T_g = 298$ K; 3.6% hexamethyl benzene-d_{18}/OS: $T_g = 297$ K; PS: $T_g = 373$ K) [13].

4. Results

Before presenting the 2D results for 26% benzene-d_6/OS, we demonstrate that the characteristic 1D two-phase spectra are also observed at low additive

concentration. In Fig. 3 1D spectra of 0.5% benzene-d_6/OS are depicted. Again, 1D two-phase spectra are observed. We mention once again that very similar 1D spectra are observed for benzene-d_6 in high molecular weight polystyrene [13].

As described in Section 2, an efficient way to elucidate the motional mechanism is to perform 2D NMR in the time domain. Fig. 4 presents the sin–sin correlation functions for the mixture 26% benzene-d_6/OS ($m_w = 1020$ g/mol) recorded using a series of evolution times t_1 at different temperatures. Only a small t_1 dependence is observed and the decay curves are characterized by very similar time constants (cf. Fig. 5). In addition, we plotted in Fig. 4 the spin–lattice relaxation function as obtained from independent measurements. At high temperatures this relaxation takes place on a longer timescale than the loss of correlation produced by the isotropic reorientation, while at $T = 133$ K the relaxation overtakes the loss of correlation so that the recorded spin alignment decay is given by the spin alignment relaxation function. Comparing the time constant of the relaxation of the Zeeman state with that of the spin alignment state, we conclude that T_1 and T_{1Q} are essentially the same. This finding will be exploited to obtain correlation functions, which are not affected by relaxation effects over the whole temperature range.

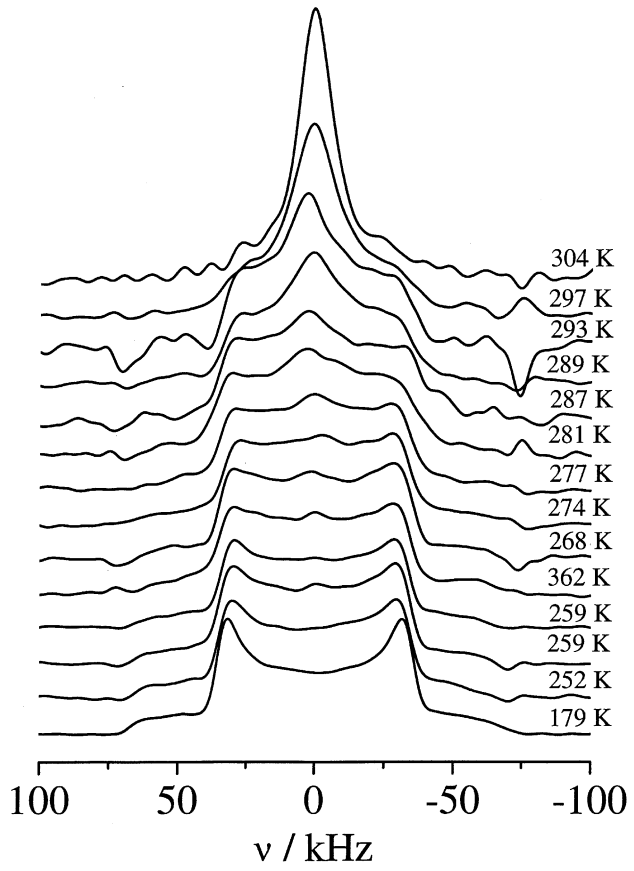

Fig. 3. 1D ^{2}H NMR spectra of 0.5% benzene-d_6/OS ($m_w = 1020$ g/mol, $T_g = 298$ K).

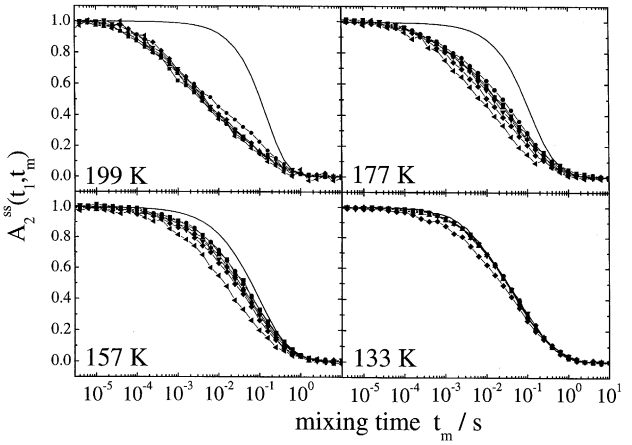

Fig. 4. Correlation functions $A_2^{ss}(t_1, t_m)$ of benzene-d_6/OS as a function of t_m ($t_1 = 3$–$250\,\mu$s, at $T = 133$ K: $t_1 = 5$–$150\,\mu$s). The solid line represents the spin–lattice relaxation function.

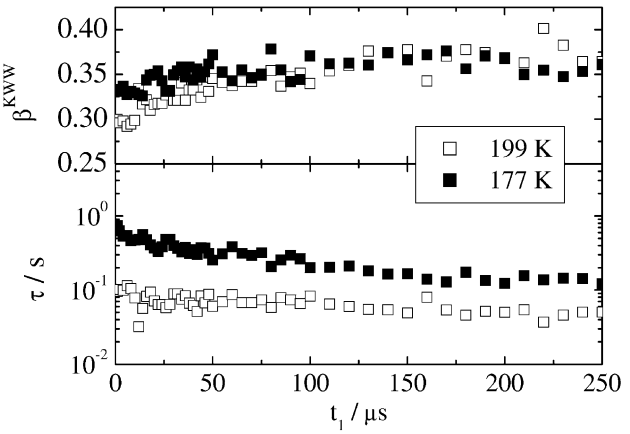

Fig. 5. Correlation time τ^{ss} of the sin–sin-correlation function $A_2^{ss}(t_1, t_m)$ and the corresponding stretching parameter β_{KWW}^{ss} of benzene-d_6/OS as a function of the evolution time t_1 for two temperatures.

The decay curves of Fig. 4 are fitted according to Eq. (15). Taking into account that the 2D spectra show isotropic reorientation, the fitting parameters $A_\infty^{ss}(t_1)$ are calculated numerically (cf. Eqs. (9) and (10)). Prior to the fitting procedure, $A_2^{ss}(t_1, t_m)$ and $A_2^{cc}(t_1, t_m)$ are corrected for relaxation effects assuming $T_{1Q} = T_1$ (cf. above). Fig. 5 presents the time constants $\tau^{ss}(t_1)$. While there is a drop at short t_1 the time constant $\tau^{ss}(t_1)$ is essentially constant at large t_1. In Fig. 6 the corresponding values $\tau^{cc}(t_1)$ extracted from the cos–cos decay curves are shown. Here, a similar behavior is observed, i.e., no significant t_1 dependence shows up for long t_1. Moreover, the time constants $\tau^{ss}(t_1)$ and $\tau^{cc}(t_1)$ are close to each other (cf. also Fig. 8). This finding will be reinspected in the discussion section. The corresponding stretching parameters $\beta^{ii}(t_1)$ (cf. Eq. (15)) of the KWW

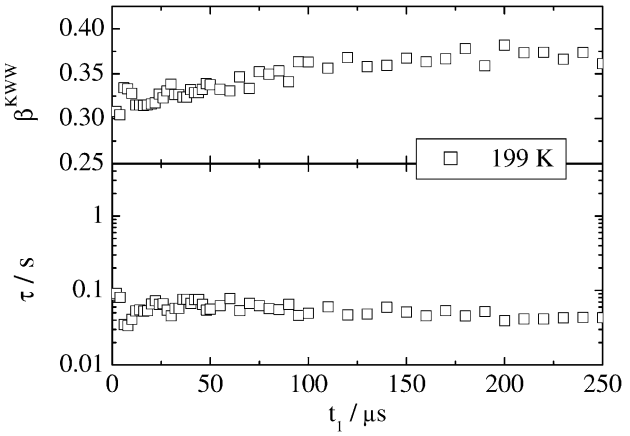

Fig. 6. Correlation time τ^{cc} of the cos–cos-correlation function $A_2^{cc}(t_1, t_m)$ and the corresponding stretching parameter β_{KWW}^{cc} of benzene-d_6/OS as a function of the evolution time t_1.

fits to the sin–sin and cos–cos curves are also displayed (cf. Figs. 5 and 6). Again only a weak t_1 dependence is recognized.

As discussed for supercooled liquids and polymers, the t_1 dependence may serve as a fingerprint of a reorientational process (cf. theory section) [6–9,26]. Here, we compare the results of benzene-d_6/OS with those obtained for the neat glass former polystyrene (present work) and glycerol [4] somewhat above T_g, cf. Fig. 7. To allow a comparison of the results, the time constants are normalized by τ_2 and the t_1 axis is scaled by the coupling constant δ (benzene/OS: 64 kHz, PS: 125 kHz, glycerol: 126 kHz). Obviously, the t_1 dependence observed for the benzene molecules in OS is different from that found for neat glass formers.

Here, some comments on the $\tau^{ss}(t_1)$ and $\tau^{cc}(t_1)$ data of the neat systems are worthwhile. For these systems the t_1 dependence for long t_1 is close to t_1^{-1} [5]. Up to our knowledge the influence of spin-diffusion on the two-time correlation functions has not yet been systematically investigated in glass forming systems. Thus, it may be possible that a crossover from a behavior determined by the molecular motion (at short t_1) to that resulting from spin diffusion (at long t_1) is observed for neat glass formers. From our point of view, further studies are needed.

With random walk simulations, assuming an appropriate motional model, the quantities $\tau^{ss}(t_1)/\tau_2$ and $\tau^{cc}(t_1)/\tau_2$ can be calculated [4,5,7,8,28]. For the random jump model—as expected from theory—no t_1 dependence is found (cf. Fig. 7). In contrast, the rotational diffusion model (approximated by jump angles $\gamma = 0.5°$) produces a strong t_1 dependence. Explicitly, one expects $\tau^{ss}(t_1) \propto t_1^{-2}$ for long evolution times [6].

Comparing the experimental data and the simulated data, one can state that the reorientation of the small benzene molecules in the binary glass former is somewhere between these two scenarios. For an isotropic reorientation, the mean jump angle $\langle\gamma\rangle$ is given by [29]:

$$\frac{\tau^{ss}(t_1 \to \infty)}{\tau_2} = \frac{3}{2}\sin^2\langle\gamma\rangle \tag{17}$$

Taking data from Fig. 7, a mean angle of about $29° \pm 2°$ results.

An appropriate jump angle distribution $P(\gamma)$ is shown in Fig. 7 (inset). The corresponding mean jump angle is about 30°. One has to keep in mind that the analysis is not unique, i.e., somehow different distributions $P(\gamma)$ may lead to similar $\tau_2^{ss}(t_1)/\tau_2$ curves. In the case of polystyrene the jump angle distribution $P(\gamma)$ is dominated by a peak at small angles (0.5°). Only a small contribution of large angles (around 20°) is found. For glycerol a bimodal distribution was found (98% 3° jumps and 2% 30° jumps) [4]. We note that for PVAc [6]

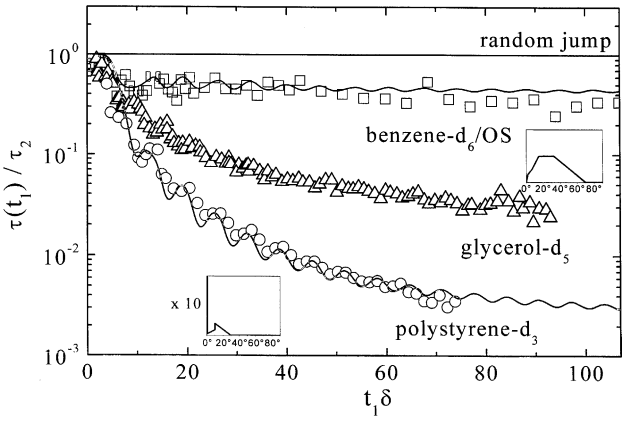

Fig. 7. t_1 dependence of the normalized correlation time τ^{ss} of benzene-d_6/OS ($T = 199$ K). For comparison data of glycerol-d_5 ($T = 203.6$ K) and polystyrene-d_3 ($T = 378$ K, τ^{cc} data) are added (data of glycerol taken from [4]). The solid lines represent fits with a distribution of jump angles $P(\gamma)$ (shown as insets).

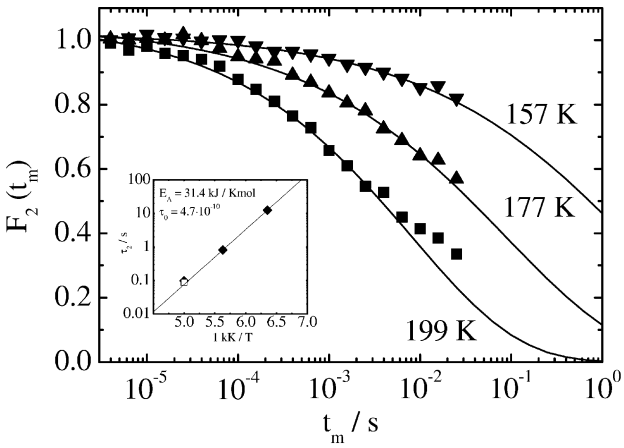

Fig. 8. Correlation function $F_2(t_m) \approx A_2^{ss}(t_1 = 3\,\mu s, t_m)$ and the corresponding time constants τ_2 of 26% benzene-d_6/OS (sin–sin, solid points; cos–cos, open symbol) as function of temperature with Arrhenius fit (solid line).

above T_g the t_1 dependence of the correlation functions, studied by ^{13}C NMR, was ascribed to a bimodal distribution of reorientation angles. Small angle ($< 0.6°$) jumps take place on a faster timescale than large angle ($\approx 10°$) jumps, so that the former give rise to a reorientation of 2° before the latter takes place. Thus, the initial drop of $\tau^{cc}(t_1)$ at short t_1 is governed by the large angle process, while a crossover to a $\tau^{cc}(t_1) \rightarrow t_1^{-1.5}$ dependence is a consequence of small angle reorientation. The $\tau^{cc}(t_1)$ curve of polystyrene (cf. Fig. 7) is similar to the

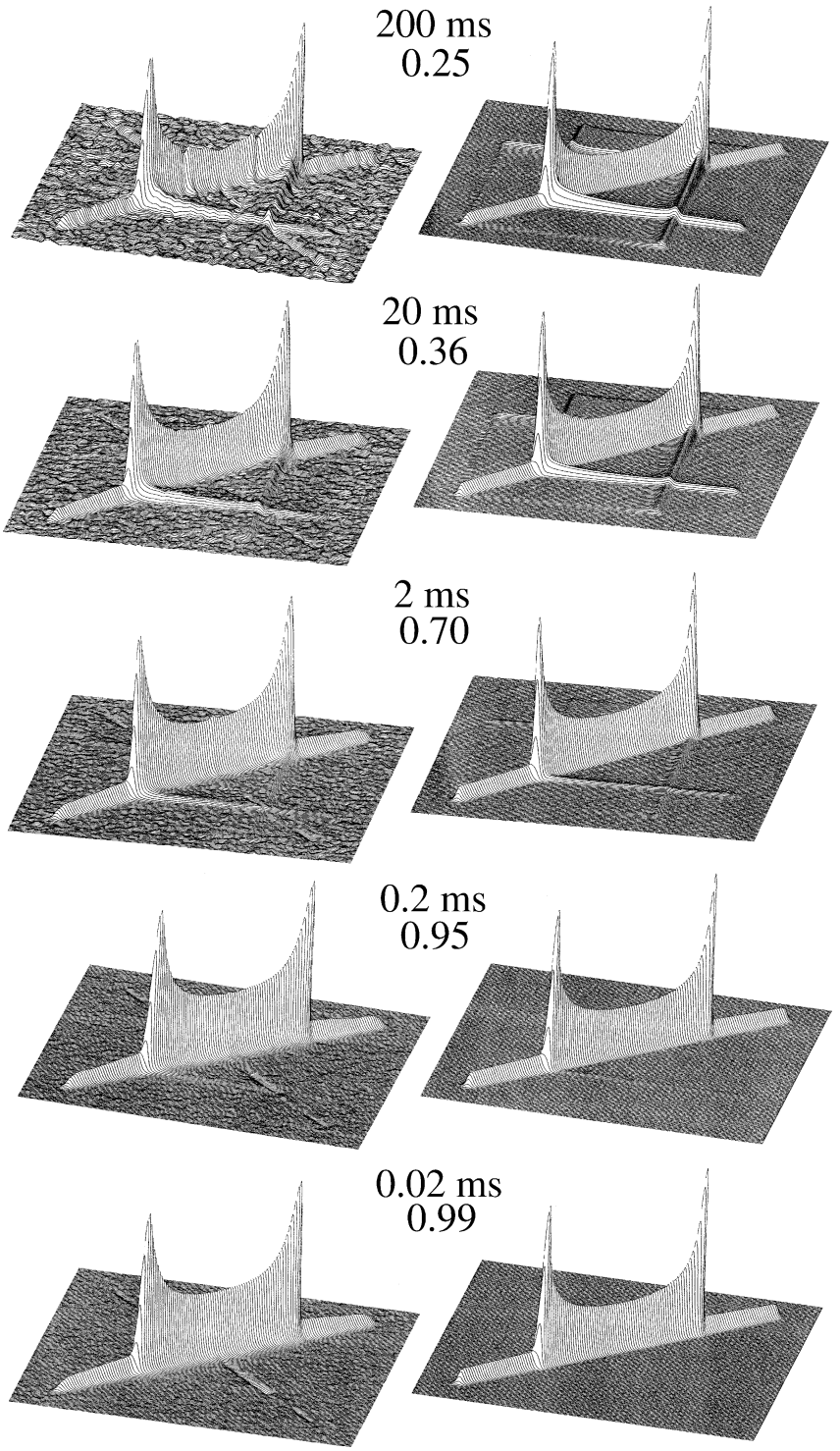

Fig. 9. t_m dependence of the ^2H 2D NMR spectra of benzene-d_6/OS. Simulations with the described 2D two-phase spectra are shown on the right-hand side.

one of PVAc. For polystyrene, a crossover to a power law for τ^{cc} at long t_1 can be observed. The corresponding exponent is -1.7.

Concerning the temperature dependence of $\tau^{ss}(t_1)/\tau_2$ and $\beta(t_1)$ (cf. Fig. 5), we note that the curves at $T = 177\,\mathrm{K}$ and $T = 199\,\mathrm{K}$ are similar. Thus, we conclude that the characteristics of the molecular reorientation do not strongly change in this temperature regime. Due to $\delta \cdot 3\,\mu s \approx 1$, $A_2^{ss}(t_1 = 3\,\mu s, t_m)$ is a good approximation of $F_2(t_m)$, after applying the T_{1Q} correction. Fig. 8 shows $A_2^{ss}(t_1 = 3\,\mu s, t_m)$ for three temperatures. The solid lines are fits (cf. Eq. (15)). The corresponding correlation time $\tau^{ss}(3\,\mu s)$ is shown in the inset of Fig. 8. The temperature dependence is described by an Arrhenius behavior with an activation energy $E_a = 31.4\,\mathrm{kJ/mol}$ and a prefactor $\tau_0 = 4.7 \times 10^{-10}\,\mathrm{s}$. For comparison, $\tau^{cc}(3\,\mu s)$ obtained from analyzing the cos–cos correlation function is included in Fig. 8. As mentioned, a very similar time constant is observed.

Above, we have demonstrated that the reorientation of the benzene molecules in the system benzene-d_6/OS results from large angle jumps, and in a fair approximation, the random jump model may apply. Then, as discussed in the theoretical section, the 2D spectra can be described by a superposition of a sub-spectrum corresponding to immobile molecules on the timescale of the mixing time t_m, namely a pure diagonal spectrum, $S_{dia}(\omega_1, \omega_2)$, and by a sub-spectrum characteristic of full isotropic reorientation, $S_{reo}(\omega_1, \omega_2)$ [2]. Inspecting the temperature dependence of the 2D spectra in Fig. 2, one indeed can anticipate this 2D two-phase model (except for the spectrum at $T = 230\,\mathrm{K}$, where an additional exchange spectrum is necessary). The t_m dependence of the 2D spectra of benzene-d_6/OS is analyzed by fitting the spectra with an additive superposition of two 2D subspectra. The results are included in Figs. 2 and 9. Clearly, the measured spectra are well reproduced. We emphasize that such a series (as function of t_m) of 2D spectra is not observed in neat glass formers or in polymers [5]. There, the initial diagonal spectrum continuously smears out when increasing the mixing time t_m [2] since small angle jumps dominate. In this case, many jumps are required for isotropization. For example, the 2D spectra of polystyrene at $T_g + 10\,\mathrm{K}$ are described by a rotational diffusion process with a broad distribution of correlation times [30]. Detailed DICO experiments at $T_g + 13\,\mathrm{K}$ [31] have shown that besides the predominating rotational diffusion large angle reorientation of the chain segments occurs. For the neat low molecular weight glass formers glycerol [4] and *o*-terphenyl [26], jump angles of some few degree were determined. A small additional contribution (<5%) of large angle (≈30°) jumps are necessary for a satisfactory description of the data.

In the case of an isotropic random jump process (cf. theory section), $W(t_m) = F_2(t_m)$ should hold. The comparison of $W(t_m)$ (cf. Fig. 9) and $A_2^{ss}(t_1 = 3\,\mu s, t_m)$, which is a good approximation of $F_2(t_m)$, is depicted in Fig. 10. Both quantities closely follow each other. The differences may be explained by deviations from a true random jump process as is found by the analysis in the time domain.

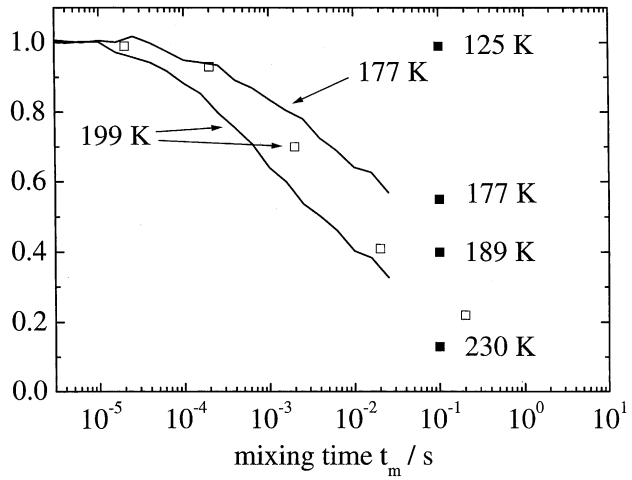

Fig. 10. Comparison between the correlation function $F_2(t_m)$ (solid line) and the 2D weighting factor $W(t_m)$ (open squares) of benzene-d_6/OS. Additional weighting factors at different temperatures are also shown (solid points).

5. Conclusions

In this contribution we have investigated binary glass formers composed of large and small molecules. The small molecules exhibit pronounced dynamical heterogeneities close to and below the glass transition temperature of the mixed system. These heterogeneities manifest themselves in characteristic 1D two-phase spectra. Binary glasses may also serve as model systems for polymer–plasticizer systems since very similar phenomena are observed. Applying 2D NMR in the time domain we have been able to clearly demonstrate that large angle reorientation, close to the limit of isotropic random jumps, takes place. We have also shown that in this case a simple analysis of the 2D spectra can be performed, since the 2D spectra are a superposition of two sub-spectra, one related to fully reoriented molecules and the other related to immobile molecules during the mixing time. Moreover, the weighting factor $W(t_m)$ is identical with the correlation function $F_2(t_m)$. We have demonstrated that the mechanism of reorientation is significantly different from the behavior in neat glass formers for which small angle reorientation dominates.

Generalizing, we want to list the experimental facts, which characterize the isotropic reorientation of the small molecules in binary glasses: (i) Reorientation of

the molecules is governed by isotropic large angle jumps. (ii) The reorientational jumps occur well below the glass transition temperature of the mixed system as determined by DSC. In the case of benzene/OS isotropic jumps on the timescale of 100 ms have been detected even 65 K below T_g [13]. (iii) In the present study, the shape of the reorientational correlation function is essentially independent of temperature, at least in the range between 177 and 199 K. (iv) The dynamical heterogeneities are transient in nature, i.e., fast moving molecules become slow and vice versa [12]. (v) The temperature dependence of the reorientational correlation time is described by an Arrhenius law. (vi) The motional heterogeneities persist even in the limit of single particle motion and we assume that similar phenomena can be observed in polymer–plasticizer systems.

The origin of such motional heterogeneities is an open question. We suggest that the effect results from translational diffusion of the small molecules in an essentially rigid matrix composed of the large molecules [5]. In other words: a given molecule moves within an energy landscape consisting of barriers of different heights. Then, each molecule changes its dynamical state from fast to slow, and vice versa, when probing the energy landscape. Large angle jumps are expected since strong orientational order is not present in glasses. The correlation time from these experiments may be connected via a hopping length to yield the macroscopic diffusion coefficient [32]. A similar mechanism has been discussed for metallic alloys, where ^{9}Be-stimulated echo decays provided atomic jump rates [33,34]. Using the same technique, slow diffusion processes of ^{7}Li ions in solid electrolyte [35] have been studied. In the case of crystalline systems rotational–translational coupling was exploited to probe defect diffusion in crystalline benzene [36]. We note that molecular jumps on a similar timescale have been observed in the glassy state by EPR experiments on spin probes [37]. In this case, the limit of tracer motion is clearly reached.

In the future, this hypothesis has to be verified, for example, by comparing the temperature dependence observed for reorientation with that of diffusion. If this idea is confirmed very slow diffusion processes occurring in disordered matrices may be studied by conventional NMR in a simple way. Of course, this model must be improved to explain the dynamics in detail, e.g., the differences between the low and high concentration systems. The model is expected to hold at least for the low concentration limit. Different phenomena such as the isotropic reorientation of molecules in "microclusters" [17] may appear when higher concentrations are studied.

Acknowledgments

We thank H. Zimmermann (Heidelberg, Germany) for preparing the deuterated hexamethyl benzene.

References

[1] C. Schmidt, S. Wefing, B. Blümich, H.W. Spiess, Chem. Phys. Lett. 130 (1986) 84.
[2] K. Schmidt-Rohr, H.W. Spiess, Multidimensional Solid-State NMR and Polymers, Academic Press, New York, 1994.
[3] F. Fujara, W. Wefing, H.W. Spiess, J. Chem. Phys. 84 (1986) 4579.
[4] R. Böhmer, G. Hinze, J. Chem. Phys. 108 (1998) 241.
[5] R. Böhmer, G. Diezemann, G. Hinze, E. Rössler, Prog. NMR Spectr. 39 (2001) 191.
[6] U. Tracht, A. Heuer, H.W. Spiess, J. Chem. Phys. 111 (1999) 3720.
[7] G. Hinze, Phys. Rev. E 57 (1998) 2010.
[8] G.R. Moran, K.R. Jeffrey, J. Chem. Phys. 110 (1999) 3472.
[9] R. Böhmer et al., J. Non-Cryst. Solids 235 (1998) 1.
[10] M. Vogel, E. Rössler, J. Chem. Phys. 114 (2001) 5802.
[11] M. Vogel, E. Rössler, J. Chem. Phys. 115 (2001) 10883.
[12] M. Vogel, E. Rössler, J. Phys. Chem. A 102 (1998) 2102.
[13] T. Blochowicz et al., J. Phys. Chem. B 103 (1999) 4032.
[14] H.A. Resing, J. Chem. Phys. 43 (1965) 669.
[15] E. Rössler, M. Taupitz, K. Börner, M. Schulz, H.-M. Vieth, J. Chem. Phys. 92 (1990) 5847.
[16] M. Vogel, P. Medick, E. Rössler, J. Mol. Liquid 86 (2000) 103.
[17] A.A. Jones, P.T. Inglefield, Y. Liu, A.K. Roy, B.J. Cauley, J. Non-Cryst. Solids 11 (1991) 556.
[18] E. Rössler, H. Spiess, H. Sillescu, Polymer 26 (1985) 203.
[19] G.P. Johari, M. Goldstein, J. Chem. Phys. 53 (1970) 2372.
[20] G. Williams, J. Non-Cryst. Solids 131–133 (1991) 1.
[21] P. Bergquist, Y. Zhu, A.A. Jones, P.T. Inglefield, Macromolecules 32 (1999) 7925.
[22] J. Jeener, B.H. Meier, P. Bachmann, R.R. Ernst, J. Chem. Phys. 71 (1979) 4545.
[23] E.N. Ivanov, Sov. Phys. JETP 18 (1964) 1041.
[24] D. Schaefer, J. Leisen, H.W. Spiess, J. Magn. Reson. 115 (1995) 60.
[25] C.P. Lindsey, G.D. Patterson, J. Chem. Phys. 73 (1980) 3348.
[26] B. Geil, F. Fujara, H. Sillescu, J. Magn. Reson. 130 (1998) 18.
[27] G. Zimmer, PhD Thesis, Univ. Mainz, 1984.
[28] G. Diezemann, R. Böhmer, G. Hinze, H. Sillescu, J. Non-Cryst. Solids 235 (1998) 121.
[29] J.E. Anderson, Environmental fluctuations and rotational processes in liquids, in: Environmental Fluctuations and Rotational Processes in Liquids, 1964.
[30] U. Pschorn et al., Macromolecules 24 (1991) 398.
[31] A. Heuer, J. Leisen, S.C. Kuebler, H.W. Spiess, J. Chem. Phys. 105 (1996) 7088.
[32] R. Kimmich, NMR: Tomography, Diffusometry, Relaxometry, Springer Press, Berlin, 1997.
[33] X.-P. Tang, R. Busch, W.L. Johnson, Y. Wu, Phys. Rev. Lett. 81 (1998) 5358.
[34] X.-P. Tang, Y. Wu, J. Magn. Reson. 133 (1998) 155.
[35] R. Böhmer, T. Jörg, F. Qi, A. Tietze, Chem. Phys. Lett. 416 (2000) 419.
[36] O. Isfort, B. Geil, F. Fujara, J. Magn. Reson. 130 (1998) 45.
[37] J.W. Saalmueller et al., J. Polym. Sci. B 34 (1996) 1093.